Kondo-like 4f delocalization in Gd at high pressure

B. R. Maddox,[1,2] A. Lazicki,[1] C. S. Yoo,[2] V. Iota,[2] M. Chen,[2] A. K. McMahan,[2] M. Y. Hu,[3] P. Chow,[3] R. T. Scalettar,[1] and W. E. Pickett[1]

[1] *University of California, Davis, California 95616*
[2] *Lawrence Livermore National Laboratory, Livermore, California 94551*
[3] *HP-CAT, Advanced Photon Source, Argonne National Laboratory Argonne, Illinois 60439*

(Dated: November 17, 2005)

We present resonant inelastic x-ray scattering (RIXS) and x-ray emission spectroscopy (XES) results which suggest Kondo-like aspects in the delocalization of $4f$ electrons in Gd metal to 113 GPa. Analysis of the RIXS data reveal a prolonged and continuous process throughout the entire pressure range, so that the volume collapse transition at 59 GPa is only part of the delocalization phenomenon. Moreover, the $L\gamma_1$ XES spectra indicate no apparent change in the bare $4f$ moment across the collapse, suggesting that Kondo screening is responsible for the expected Pauli-like behavior in magnetic susceptibility.

PACS numbers: 62.50.+p, 61.10.-I, 64.70.Kb, 64.30.+t

A number of compressed lanthanide and actinide metals exhibit electron correlation driven phase transitions characterized by unusually large volume changes [1–3]. Among the lanthanides, such volume collapse transitions are seen in Ce (15%), Pr (10%) , Gd (5%), and Dy (6%) at pressures of 0.7 [4], 20 [5] , 59 [6], and 73 GPa [7], respectively. It is often presumed that the $4f$ electrons delocalize across these collapse transitions due to dramatic changes in properties seen on going from the large- to small-volume regimes. The crystal structures change from a high-symmetry sequence observed in metals without f electrons, to generally low-symmetry early-actinide-like structures indicating f-bonding [1–3]. The magnetic susceptibility changes from Curie-Weiss behavior reflecting the Hunds rules moments to an expected temperature-independent Pauli-like paramagnetism suggesting loss of the moments [2, 4]. On the other hand, it has been recently shown that Nd reaches a typically itinerant α-U structure through a sequence of transitions without any large volume changes [8]. Additionally, high-energy neutron scattering measurements see single-ion magnetic response in α Ce [9] in possible disagreement with the result from magnetic susceptibility [4]. It would appear that delocalization in these f-electron metals is not fully understood.

There are presently two viable theoretical perspectives which reflect some of these same conflicts. The Kondo volume collapse (KVC) model for Ce attributes the collapse to a region of rapid change in the Kondo binding energy associated with screening of the $4f$ moments by the valence electrons [10, 11]. While this occurs near the localized limit (large volume) for Ce, implicit in the model is also a prolonged delocalization in the way that the ground state evolves away from sharp f^1 character as volume is reduced. Dynamical mean-field theory (DMFT) calculations generally find Kondo-like features in both lanthanides [13] and actinides [14], and specifically support the KVC model for Ce [12], although not necessarily for the other f-electron metals [13]. The Mott transition model [15], as exemplified by local density calculations modified to represent the localized regime by spin and orbitally polarized solutions, presents a more abrupt change from localized to itinerant behavior across the collapse transitions, coincident with complete loss of the f-moment itself [16–18].

Recent developments in 3^{rd} generation synchrotron x-ray spectroscopies offer new opportunities to clarify the mechanism of delocalization in the f-electron metals. The present paper reports resonant inelastic x-ray scattering (RIXS) and x-ray emission spectroscopy (XES) measurements on Gd metal up to 113 GPa, both of which have been used successfully in probing the electronic and magnetic properties of materials [19–24]. The results strongly support a Kondo-like scenario by showing (1) a prolonged and continuous (as a function of volume) delocalization of the $4f$ electrons throughout the full pressure range investigated and (2) a $4f$-moment which does not change at the 59 GPa volume collapse. As in the high-energy neutron scattering results for the collapsed α phase of Ce [9], it is argued that the XES process measures a bare $4f$ moment, and that any moment loss deduced from the magnetic susceptibility must then come from screening by the valence electrons.

High purity Gd foil (99.99%, Alpha Aesar) was loaded into a LLL-type DAC, using 200 μm flat diamond-anvils and Be as the gasket material, together with mineral oil as a pressure medium and ruby as a pressure marker. X-ray spectroscopic data was collected at Sector 16 ID-D at the Advanced Photon Source, using an x-ray beam microfocused to 20×50 μm by a pair of 1 m long Kirkpatrick-Baez mirrors. For RIXS experiments we tuned the incident x-ray energy, Ω, through the L_{III} absorption edge from 7.235 KeV to 7.257 KeV in steps of 2 eV using a diamond double-crystal monochromator. At each incident

energy, we collected the $L\alpha_1$ emission spectra at 90° from the incident x-ray over a 100 eV energy range. Both the incident and emitted x-ray photons were sent through the Be gasket to minimize signal loss due to diamond absorption. Furthermore, the cell was tilted to $\sim 7°$ from the horizontal plane to increase the physical cross section of the sample and to minimize the effects of self-absorption. For XES we used an incident monochromatic (12 KeV) x-ray beam and collected the $L\gamma_1$ x- ray emission (7.786 KeV) at 90° from the incident x-ray through the Be gasket. In both cases energy analysis was performed using a 1 m Rowland circle spectrometer arranged in the vertical plane using Gd foil for calibration. A spherically bent Si(333) single crystal analyzer (100 μm in diameter) was used to refocus the x-ray emission onto a Si detector (Amp Tek). This configuration provides an energy resolution of approximately 1 eV.

Figure 1 shows a typical two-dimensional RIXS scan at 18 GPa plotted as a function of the incident x-ray and the energy transfer to the outgoing fluorescence, ω, labeled $(\Omega - \omega)$. These spectra are qualitatively similar to those previously obtained from $Gd_3Ga_5O_{12}$ garnet at ambient pressure [20]. The main features of the spectra are associated with two transitions as illustrated in the inset: a strong dipole-allowed(E1) $2p \rightarrow 5d$ transition resonant at $\Omega = 7.247$ KeV (marked in blue) and a substantially weaker quadrupolar(E2) $2p \rightarrow 4f$ transition which resonates at $\Omega = 7.239$ KeV (marked in red) . The energy transfers of these two transitions after the $L\alpha_1$ $3d \rightarrow 2p$ core-hole decay are identified at $(\Omega - \omega) = 1.187$ KeV and 1.179 KeV, respectively, representing the $3d \rightarrow 5d$ (blue dotted line) and $3d \rightarrow 4f$ (red dotted line) M-band absorption spectra normally impossible to measure at high pressures by ordinary x-ray absorption measurements. A broad feature at ~ 1.195 KeV, marked as B* in Fig. 1 exhibits the same resonance characteristics as peak B and is therefore is part of the same multiplet group as B [20]. The main peak at $(\Omega - \omega) = 1.187$ KeV shows a slight shift with incident energy. This shift is caused by two multiplet groups separated by ~ 1 eV in strong crystal fields which resonate at slightly different W. Excitations above $\Omega = 7.247$ KeV correspond to excitations into continuum states and represent non-resonant XES. Note that the low-energy $2p \rightarrow 4f$ quadrupolar transition, normally hidden in normal x-ray absorption spectroscopy by the much stronger core-hole broadened $2p \rightarrow 5d$ absorption, is easily observed using RIXS.

Dramatic changes are observed in the RIXS spectra with increasing pressure as summarized in Fig. 2. As made clear by the Gaussian decompositions of the $\Omega = 7.239$ KeV spectra, a new feature (red hatched, C) arises strongly at 4.96 eV below the main group as pressure increases. By 113 GPa, its intensity has increased considerably to roughly 2/3 that of the main feature, peak B, suggesting that this new feature arises via a dipole allowed transition to the intermediate state. The

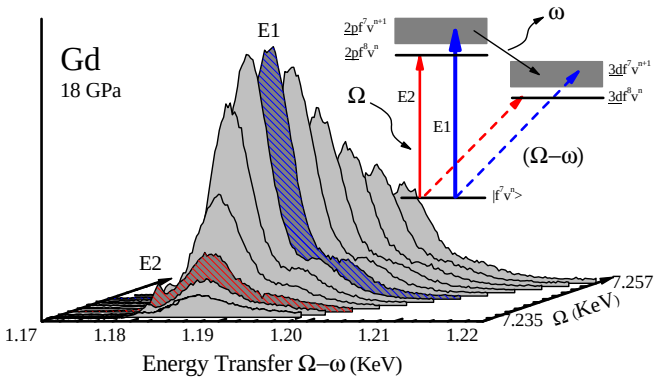

FIG. 1: (color online) RIXS spectra of Gd at 18 GPa taken at a series of incident energies from $\Omega = 7.235$ KeV to $\Omega = 7.257$ KeV in steps of 2 eV. The inset shows a schematic energy diagram indicating the RIXS process for $3d \rightarrow 4f$ (A) and $3d \rightarrow 5d$ (B) (dotted lines) via the resonant L_{III} absorption bands of $2p \rightarrow 5d$ (E1) at $\Omega = 7.247$ keV and $2p \rightarrow 4f$ (E2) at $\Omega = 7.239$ KeV (solid lines).

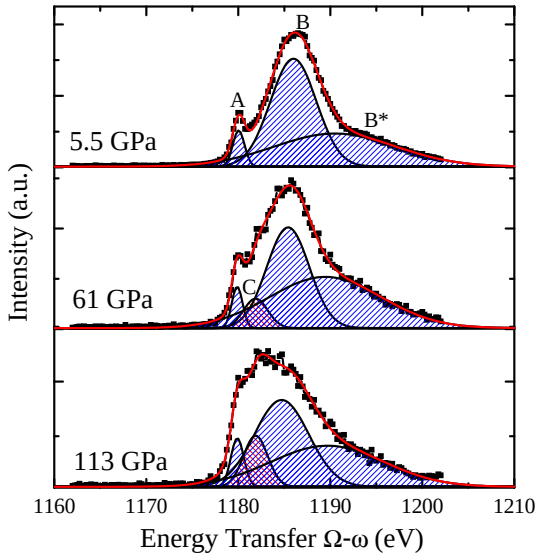

FIG. 2: (color on line) The RIXS spectra obtained at the $2p \rightarrow 4f$ resonance at $\Omega = 7.239$ keV to 113 GPa, together with their Gaussian decompositions. Peaks A and B are assigned in Fig. 1. Peak B* arises from the same multiplet as with peak B [20]. Note that peak C at 1182 eV (red hatched) grows strongly with pressure and arises via dipole transitions to intermediate states.

characteristics of this new feature in energy, intensity, and bandwidth are strikingly similar to those previously observed in the pressure-induced intermediate valence of YbS (f^{14} in Yb^{+2} and f^{13} in Yb^{+3}) [25], and with the larger f^2 peak for α as compared to γ phases of Ce alloys at ambient pressure [21, 22].

The present Gd situation is analogous to the Ce case [21, 22], and illustrated by the ground state wavefunction

$$|\Psi\rangle = \alpha|4f^7v^3\rangle + \beta|4f^8v^2\rangle + \gamma|4f^6v^4\rangle \qquad (1)$$

where v signifies valence electrons. In the strongly localized limit, the occupation of the $4f$ shell in Gd is pinned at f^7. Under compression, however, the growing f-valence hybridization increasingly favors fluctuations of the $4f$ electrons into valence states, and vice versa, resulting in the growth of f^6 and f^8 components of the wavefunction at the expense of the predominant f^7 character. The $f-f$ hybridization has a similar effect. This type of delocalization differs from intermediate valence where one stays near the localized limit except that the energies of two different f occupations happen to move closer together as a function of a variable like pressure. However, the RIXS process for these two phenomena are similar in that the $4f$core-hole attraction in the intermediate state puts the peak arising from dipole excitation of the component with larger f occupation ($\underline{2p}4f^8v^3$, C) at lower energy transfer than that of the smaller occupation ($\underline{2p}4f^7v^4$, B). Indeed, the interpretations and relative locations of all three peaks, A(E2), B (E1), and C(E1), are consistent with the YbS intermediate valence case (Fig. 4b, [25]). The f^6 term in Eq.(1) does imply a fourth $\underline{2p}4f^6v^5$ peak at energies above Peak B, however, it is difficult to resolve this from our data.

The RIXS spectra quantify the progress of 4f delocalization in compressed Gd by $|\gamma|^2/|\beta|^2 \approx n(f^8)/n(f^7)$. This ratio was extracted from our data by first normalizing each $\Omega = 7.239$ keV spectra by total area and then subtracting our lowest pressure spectra, taken at 5.5 GPa, from each of the higher pressure scans. The remaining positive peak in the difference spectra was integrated to get and an area A and the quantity $n(f^8)/n(f^7) \approx A/(1-A)$ was then calculated. The results are plotted in Fig. 3 as a function of volume, along with recent DMFT results for Ce [13] and experimental values for ambient-pressure α and γ phases of Ce alloys also obtained from RIXS [21]. In both cases the two volume-collapse regions are shaded. The present data show an approximately continuous and exponential dependence on volume as predicted by theory [13], with the $n(f^{n+1})/n(f^n)$ ratio for Gd ($n = 7$) lying far below that of Ce ($n = 1$) and its compounds.

One would expect Gd to be more localized and thus have a smaller $n(f^{n+1})/n(f^n)$ ratio than Ce at the same volume since the f shell is more tightly bound in the heavier lanthanides due to the increasing but incompletely screened nuclear charge. More important is the half-filled shell in Gd with total $4f$ spin $S = 7/2$ and the associated large impact of the intraatomic exchange. This is reflected in a ~ 12 eV splitting (an effective Hubbard U) between lower and upper Hubbard bands in Gd as compared to ~ 6 eV in Ce [26], which should make Gd significantly more localized. It is interesting to note that the volume collapse transitions (shaded regions) occur in roughly the same range of $n(f^{n+1})/n(f^n)$ as measured by RIXS in both Gd and Ce.

We have also examined the f-electron moment by us-

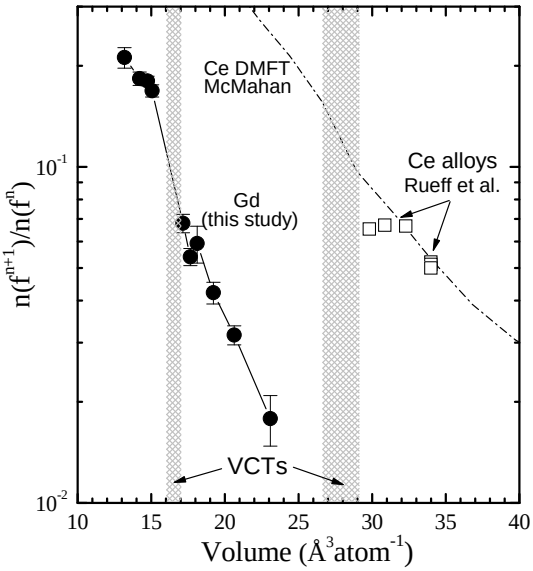

FIG. 3: The degree of f-electron hybridization, reflected by the ratio f^{n+1}/f^n,measured by the present RIXS experiments on Gd compared with those previously determined in RIXS experiments on Ce alloys and in recent DMFT calculations. The volume collapse transition (VCT) regions for Gd and Ce are shown as hatched areas.

ing $2p4d$ $L\gamma_1$ XES measurements on Gd in the DAC. The intraatomic exchange interactions between $4f$ and core orbitals lead to a low energy satellite as seen in Fig. 4, whose relative height and separation from the main peak should reflect the size of the $4f$ moment [23]. We find no significant change in the $L\gamma_1$ emission spectra up to 106 GPa, the highest pressure attained in this study, suggesting no changes in the $4f$ moments up to this pressure and in particular, no changes across the collapse transition at 59 GPa. The inset in Fig. 4 shows the relative height of the satellite to main peak obtained from *ab intio* atomic calculations of the XES process for Gd, carried out for the lowest-energy states of the $4f^7$ shell for each of $J = 1/2$, $3/2$, $5/2$, and $7/2$ [27]. This ratio will be smaller in the solid due to screening of the intraatomic exchange interactions. However, the essential message here is that theory predicts that changes away from the $J = 7/2$ $^8S_{7/2}$ Hunds rules ground state should result in significant changes in the XES spectra which are not seen experimentally. We find the same null behavior across the collapse transition in Pr. This behavior in both Gd and Pr is in contrast to the essentially complete loss of Mn $3d$ moment across the Mott transition in MnO as probed by similar $1s3p$ $K\beta$ XES measurements [24].

As noted earlier, measurements of magnetic susceptibility in a Ce and early actinide analogs has led to the expectation of a temperature-independent magnetic susceptibility in the collapsed phases of the f-electron metals, suggesting the absence of moments [2, 4]. Yet the single-ion magnetic response seen in high-energy neutron

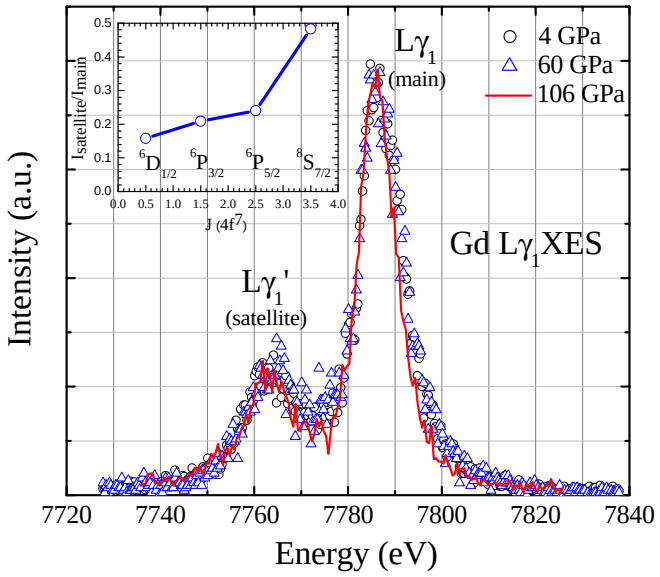

FIG. 4: (color on line) $L\gamma_1$ XES spectra of Gd at 4, 65, and 106 GPa, normalized to the main peak intensity, showing no apparent change in the $L\gamma_1'$ satellite peak intensity, suggesting no changes in the $4f$ moments up to 106 GPa. For comparison, we present simulated $L\gamma_1$ spectra, shown in the inset, clearly demonstrating that the ratio $I_{satlellite}/I_{main}$ decreases as you move away from the Hunds rule ground state.

scattering measurements for α-Ce is consistent with a still extant $4f$ moment [9], a dilemma which is resolved by the Kondo perspective that the susceptibility measures a $4f$ moment largely screened away by the valence electrons [10, 11]. It seems intuitively clear that the primarily atomic XES process, which reflects exchange interactions between $4f$ and core-hole orbitals whose radial distributions lie generally closer to the nucleus than do those of the valence orbitals, is also measuring a bare $4f$ moment. The persistence of such bare $4f$ moments in Gd and Pr through the collapse transitions is therefore consistent with Kondo-like behavior.

In summary, f-electron delocalization is brought about by growing hybridization which causes increasing fluctuations away from the sharp f^n character of the localized limit, and the degree of hybridization can be quantitatively probed by RIXS even at pressures over 100 GPa. As seen here for f^7 Gd, this process is prolonged and continuous as a function of volume. This in turn suggests that the volume collapse transition is only part of the phenomenon and acts to accelerate the delocalization. The present XES results suggest that the bare $4f$ moments persist across such collapse transitions in Gd and Pr, and also in Nd where these is no such collapse, so that any loss of temperature dependence in the magnetic susceptibility must then arise from Kondo-like screening of these moments.

This work has been supported by the LDRD-04-ERD-020 and PDRP programs at the LLNL, University of California, under the auspices of the U.S. DOE under Contract No. W-7405-ENG-48 and by the Stewardship Science Academic Alliances Program under grant DOE DE-FG03-03NA00071. Use of the HPCAT facility was supported by DOE-BES, DOE-NNSA (CDAC, LLNL, UNLV), NSF, DOD-TACOM, and the W. M. Keck Foundation.

[1] W. B. Holzapfel, J. Alloys Compd. **223**, 170 (1995).
[2] A. K. McMahan et al., J. Comp. Aided Mat. Des. **5**, 131 (1998).
[3] A. Lindbaum et al., J. Phys.: Condens. Matter **75**, S2297 (2003).
[4] D. G. Kiskimaki and J. K. A. Gschneidner, *Handbook on the Physics and Chemistry of Rare Earths* (North-Holland, Amsterdam, 1978).
[5] B. J. Baer et al., Phys. Rev. B **67**, 134115 (2003); N. C. Cunningham et al., Phys. Rev. B **71**, 012108 (2005).
[6] H. Hua, Y. K. Vohra, and J. Akella, Rev. High Pressure Sci. Technol. **7**, 233 (1988).
[7] R. Patterson, C. K. Saw, and J. Akella, J. Appl. Phys. **95**, 5443 (2004).
[8] G. N. Chesnut and Y. K. Vohra, Phys. Rev. B **61**, R3768 (2000).
[9] A. P. Murani et al., Phys. Rev. B **15**, 5890 (1977).
[10] J. W. Allen and R. M. Martin, Phys. Rev. Lett. **49**, 1106 (1982).
[11] M. Lavagna, C. Lacroix, and M. Cyrot, Phys. Lett. **90A**, 210 (1982).
[12] K. Held, A. K. McMahan, and R. T. Scalettar, Phys. Rev. Lett. **87**, 276404 (2001); M. B. Zölfl et al., Phys. Rev. Lett. **87**, 276403 (2001).
[13] A. K. McMahan, Phys. Rev. B **72**, 115125 (2005).
[14] S. Y. Savrasov, G. Kotliar, and E. Abrahamas, Nature **410**, 793 (2001).
[15] B. Johansson, Philos. Mag. **30**, 469 (1974).
[16] O. Eriksson, M. S. S. Brooks, and B. Johansson, Phys. Rev. B **41**, R7311 (1990).
[17] A. Svane et al., Phys. Rev. B **56**, 7143 (1997).
[18] P. Soderlind and A. Landa, Phys. Rev. B **72**, 024109 (2005).
[19] A. Kotani and S. Shin, Rev. Mod. Phys. **73**, 203 (2001); A. Kotani, Eur. Phys. J. B **47**, 3 (2005);
[20] M. H. Krisch et al., Phys. Rev. Lett. **74**, 4931 (1995).
[21] J.-P. Rueff et al., Phys. Rev. Lett. **93**, 67402 (2004).
[22] C. Dallera et al., Phys. Rev. B **70**, 085112 (2004).
[23] K. Jouda, S. Tanaka, and O. Aita, J. Phys. Cond. Matt. **9**, 10789 (1997).
[24] C. S. Yoo et al., Phys. Rev. Lett. **94**, 115502 (2005).
[25] C. Dallera et al., J. Phys.: Condens. Matter **17**, S849 (2005).
[26] Y. Baer and W. D. Schneider, *Handbook on the Physics and Chemistry of Rare Earths*, vol. 10 (Elsevier Science, 1987).
[27] The $2p4d$ XES process for an isolated Gd atom was calculated using a fully relativistic multiconfiguration Dirac-Fock code with the $4f^7$ shell in its lowest energy state for $J = 1/2$, $3/2$, $5/2$, and $7/2$, and taking a $J = 1/2$ $2p$ core hole.